UC Santa Cruz

UC Santa Cruz Previously Published Works

Title

Stereochemical determination and bioactivity assessment of (S)–(+)-curcuphenol dimers isolated from the marine sponge Didiscus aceratus and synthesized through laccase biocatalysis

Permalink

Journal

ISSN

Authors

Cichewicz, Robert H
Clifford, Laura J
Lassen, Peter R
et al.

Publication Date

DOI

Copyright Information

Peer reviewed

Graphical abstract for the manuscript:

Stereochemical determination and bioactivity assessment of (*S*)-(+)-curcuphenol dimers isolated from the marine sponge *Didiscus aceratus* and synthesized through laccase biocatalysis.

Robert H. Cichewicz,[a,b] Laura J. Clifford,[a,b] Peter R. Lassen,[c,†] Xiaolin Cao,[c] Teresa B. Freedman,[c] Laurence A. Nafie,[c] Joshua D. Deschamps,[a] Victor A. Kenyon,[a] Jocelyn R. Flanary,[a,b] Theodore R. Holman,[a,*] Phillip Crews[a,b,*]

Sponge: *Didiscus aceratus*

Vibrational Circular Dichroism

Atropisomers

1

Stereochemical determination and bioactivity assessment of (*S*)-(+)-curcuphenol dimers isolated from the marine sponge *Didiscus aceratus* and synthesized through laccase biocatalysis.

Robert H. Cichewicz,[a,b] Laura J. Clifford,[a,b] Peter R. Lassen,[c,†] Xiaolin Cao,[c] Teresa B. Freedman,[c] Laurence A. Nafie,[c] Joshua D. Deschamps,[a] Victor A. Kenyon,[a] Jocelyn R. Flanary,[a,b] Theodore R. Holman,[a,*] Phillip Crews[a,b,*]

[a]*Department of Chemistry and Biochemistry and* [b]*Institute for Marine Sciences, University of California, Santa Cruz, CA 95064, U.S.A.*
[c]*Department of Chemistry, Syracuse University, Syracuse, NY 13244, U.S.A.*

Abstract. Electrospray ionization mass spectrometry-guided isolation of extracts from *Didiscus aceratus* led to the discovery of several new derivatives of the bioactive bisabolene-type sponge metabolite (*S*)-(+)-curcuphenol (**1**). The compounds obtained by this method included a mixture of known (**2**) and new (**3**) dihydroxylated analogs as well as a novel family of dimeric derivatives, dicurcuphenols A – E (**4** – **8**), and dicurcuphenol ether F (**9**). Dimers **4** – **9** were also subsequently obtained through a hemi-synthetic method in which **1** was incubated with the enzyme laccase. Atropisomeric dimers **5** and **6** were subjected to vibrational circular dichroism (VCD) analysis thereby establishing their absolute biaryl axial chirality as *P* and *M*, respectively. In contrast to **1**, metabolites **2** – **9** exhibited weak or no cytotoxic or lipoxygenase inhibitory effects.

*To whom correspondence should be addressed. P.C. Tel: 831-459-2603. Fax: 831-459-2935. E-mail: phil@chemistry.ucsc.edu; T.R.H. Tel: 831-459-5884. Fax: 831-459-2935. E-mail: holman@chemistry.ucsc.edu.

†Visiting from Quantum Protein Center, Department of Physics, Technical University of Denmark, DK-2800 Lyngby, Denmark.

INTRODUCTION

Bisabolene-type sesquiterpenoids constitute a class of broadly active natural products biosynthesized by a diverse range of organisms from both terrestrial and marine habitats. Within the marine environment alone, numerous bisabolene sesquiterpenoids have been reported from sponges (*Acanthella*,[1] *Arenochalina*,[2] *Axinyssa*,[3] *Ciocalypta*,[4] *Didiscus*,[5,6] *Epipolasis*,[7,8] *Halichondria*,[9] *Haliclona*,[10] *Myrmekioderma*,[11] and *Theonella*[12,13]), a nudibranch,[14] gorgonians,[15,16,17,18] a sea hare,[19] and red algae.[20,21] Included among these discoveries are a number of uniquely functionalized bisabolene species such as heterocyclic,[10] nitrogenous,[3,4,9,13] halogenated,[19] poly-hydroxylated quinone,[15] and acetylated[20] derivatives that have significantly broadened the biosynthetic scope of this distinct chemical family. It is of particular interest to note that two unique classes of bisabolene-type metabolites are recognized based on their C-7 absolute stereochemistry. As previously described,[10] all known sponge-derived bisabolenes possess a 7*S* configuration while the remaining marine and terrestrial metabolites exhibit a 7*R* configuration.

The lead compound of this family, (*S*)-(+)-curcuphenol (**1**) ($C_{15}H_{22}O$), has attracted much attention due to its distribution among marine sponges and biological activities. This compound has been encountered as a major sesquiterpene metabolite (yield >1 % dry weight) in four sponge genera (*Arenochalina*,[2] *Didiscus*,[5,6] *Epipolasis*,[7,8] and *Myrmekioderma*[11]) from the Caribbean,[5,6,8,11] western Australia,[2] and Japan.[11] In contrast, the marine occurrences of the optical antipode of **1**, (*R*)-(-)-curcuphenol, have been limited to several New World gorgonians from the genus *Pseudopterogorgia*.[15,16,18] These compounds are reported to possess numerous biological effects including antimicrobial,[5,6,18] H/K-ATPase inhibitory,[7] antiplasmodial,[5] and cytotoxic activities.[22] In light of these promising findings, we believed that the search for novel derivatives of **1** would be rewarding. It could provide opportunities to explore new structural themes and further probe the pharmacological activities in this family of bioactive metabolites.

Herein, we report on the discovery of a unique branch in this family of sponge-derived curcuphenol metabolites based on ESIMS screening of extracts. The goal of the project was to engage in the structure elucidation, absolute configuration analysis,

cytotoxicity, lipoxygenase inhibition, and active site modeling of the new compounds encountered. Further insights addressing the biogenic origin of the curcuphenol-derivatives are also addressed. Additionally, we highlight the first application of vibrational circular dichroism (VCD)[23] to the stereochemical analysis of marine natural products. Traditional UV-circular dichroism studies, as exemplified by numerous scholarly studies performed by Professor Koji Nakanishi and colleagues,[24,25] have greatly enhanced the field of stereochemical analysis in organic chemistry. Our studies serve as an extension of these insightful efforts via the application of contemporary VCD analysis methodologies that should serve to compliment traditional UV-CD techniques.

RESULTS AND DISCUSSION

Summary of Compounds Studied. Sponges from the western Indo Pacific have continued to serve as a source of unique and bioactive secondary metabolites. Many of the specimens in our extensive collection have been subjected to preliminary bioactivity screening with a simple brine shrimp assay.[26] Partitioning of the total crude organic extract of *Didiscus aceratus* (Ridley and Dendy)[27] yielded a CH_2Cl_2 soluble fraction that exhibited potent toxicity against brine shrimp (100% lethality in ~20 min, 10 μg/mL). Bioassay guided isolation of the active fraction provided (*S*)-(+)-curcuphenol (**1**) (Figure 1) identified by its HRESIMS (*m/z* 219.1746 [MH]$^+$, calcd for $C_{15}H_{23}O$, 219.1749), NMR data, and optical rotation value.[6,7] Studies of the cancer cell cytotoxicity of compound **1** were performed as previously described.[28] These data revealed that **1** possessed moderate, but nonspecific toxicity against human bone marrow, leukemia, and colon solid tumor cell lines as observed earlier for similar curcuphenol analogs[22] and therefore was not pursued for subsequent in vivo evaluation.

Interestingly, further consideration of the planar structure of **1** revealed that it shared several key features with other marine biomolecules previously isolated by our laboratory that exhibited potent inhibition against human lipoxygenases.[29,30,31,32] These attributes included (i) a polar phenolic head-group, (ii) a lipophilic tail, (iii) moderate cLogP value (4.9), and (iv) probable redox activity. In view of these features, compound **1** was tested and determined to be a potent, but non-selective inhibitor of human

lipoxygenases (human 12-lipoxygenase: IC_{50} 2.9 ± 0.4 µM and human 15-lipoxygenase: IC_{50} 1.6 ± 0.3 µM).

The overwhelming presence of **1** in the *D. aceratus* extracts (>8% of total crude extract) precluded the direct bioassay-guided isolation of related analogs from the remaining fractions due to the masking effects of **1**. Another approach based on ESIMS analysis of the sponge extracts was utilized to systematically screen for the presence of analogs of compound **1**. It was anticipated that these compounds would help compliment our growing library of marine-derived human lipoxygenase inhibitors and shed further light on key structure-activity-relationships of these biomolecules. Consequently, two fractions were identified that exhibited *m/z* 253 [MH]⁺ ($C_{15}H_{25}O_3$) and 435 [MH]⁺ ($C_{30}H_{43}O_2$) representing dihydroxylated and dimeric curcuphenol species, respectively. Subsequent ESIMS-guided isolation led to the purification of a mixture of the known 10*β*-hydroxycurcudiol[5] (**2**) and new 10*α*-hydroxycurcudiol (**3**) as well as six curcuphenol dimers, dicurcuphenols A – E (**4 – 8**) and dicurcuphenol ether F (**9**) (Figure 1).

Insert Figure 1

Structure Determination of Compounds 2 – 9. Compounds **2** and **3,** obtained as a mixture, were not further separated because their characterization as 10-hydroxycurcudiol (syn. 10,11-dihydroxycurcuphenol) diastereomers was straightforward. The HRESIMS (obs *m/z* 253.1800; calcd for $C_{15}H_{25}O_3$, 253.1804) of the single HPLC peak containing **2** and **3** indicated two OH groups had been added to the curcuphenol (**1**) skeleton. Further attempts at separating **2** and **3** by HPLC provided inadequate resolution of the metabolites; therefore, structure determination proceeded with the mixture. Inspection of the ¹H, ¹³C, and DEPT NMR spectra of the mixture confirmed the presence of 10*β*-hydroxycurcudiol (**2**) that was previously reported as a microbial biotransformation product of **1**.[5] A second set of closely aligned peaks of equivalent intensity was also noted in the NMR spectra. Careful examination of these proton and carbon spins indicated that they were derived from the C-10 epimer of **2**, 10*α*-hydroxycurcudiol (**3**).

The remaining compounds, **4 – 9**, were isomeric dimers that each exhibited *m/z* 435 [MH]$^+$ by low-resolution MS. Their molecular formulas were subsequently established as $C_{30}H_{42}O_2$ by HRESIMS. Compared to curcuphenol (**1**), this represented nearly double the number of carbon (2×15C), hydrogen (2×22H-2H), and oxygen (2×2O) atoms expected for two units of monomeric **1**. The loss of 2H atoms was determined to arise from the formation of a new covalent bond indicating that **4 – 9** were dimeric metabolites of **1**. An initial assessment of the ^{1}H NMR spectra of **4 – 9** confirmed these metabolites exhibited analogous spectral features to **1** thereby establishing their common curcuphenol-derived skeleton. Most of the upfield ^{1}H NMR peaks appeared doubled in **4 – 9** compared to **1**; however, the downfield aromatic resonances of the dimers differed significantly both in the absence of key proton spins and/or divergent chemical shifts indicating that dimerization had occurred through the aryl portion of **1**. The structure elucidation of **4 – 9** was greatly supported via utilization of the comparative ^{1}H NMR spectra as illustrated in Figure 2. Further confirmation of these assignments was achieved by ^{13}C NMR and HMQC/HMBC experiments focusing on the downfield spectral region in order to discern the unique aryl linkages of these six dimers.

Insert Figure 2

The benzenoid protons of dicurcuphenol A (**4**) appeared as singlets (δ 6.90, 6.87, 6.68, and 6.67) versus the doublets observed in the aromatic region for **1** (H-4 to H-5 coupling). This indicated that the two possible dimerization sites were either at the C-4 or C-5 positions of **1**. Thus, three possible dimers were envisioned with the aryl linkages being between positions C-4 to C-4′, C-5 to C-5′, or C-4 to C-5′/C-4′ to C-5. All of the non-aromatic-ring NMR signals of **4** could be correlated to resonances of **1** including C-7 to C-15. Subsequent detailed analysis of selected elements from 1D and 2D NMR data were required to distinguish among the three alternatives for the dimer skeleton.

The choice in favor of C-4 to C4′ dimerization in **4** was made as outlined below. The ^{13}C resonances assigned to C-4 and C-4′ (δ 134.8, two quaternary C's) were significantly shifted downfield (Δδ ~ 12) relative to C-4 of **1**, and protons H-5 and H-5′ (both singlets) in **4** were shifted upfield relative to that of the H-5 doublet in **1** as

7

illustrated in Figures 2b and 2a, respectively. The most important $^{2-3}J_{H-C}$ data shown in Figure 3 consisted of distinct three-bond HMBC correlations observed between H-7/C-5, H-15/C-4, H-7′/C-5′, and H-15′/C-4′. Both of the alternate dimeric structures considered at the outset were ruled out because several of these HMBC correlations would span across four-bonds. Further HMBC correlations were ambiguous due to the coincidental overlap of carbon resonances.

Insert Figure 3

Once separated, it was clear that subtle structural features were responsible for the diastereomeric differences between dicurcuphenols B (**5**) and C (**6**). For example, the downfield resonances in the ^{1}H NMR spectra for **5** and **6** exhibited identical multiplet patterns with very similar chemical shifts as shown in Figure 2c versus 2d, respectively. However, this pair exhibited unique optical rotatory properties with $[\alpha]^{25}_D = 103.0°$ for **5** and $[\alpha]^{25}_D = 2.87°$ for **6**. The downfield ^{1}H NMR data in Figures 2c and 2d revealed that **5** and **6** possessed biaryl linkages quite different from that of **4**. Two connectivity arrangements were possible for **5** and **6** based on the multiplet patterns observed for the aryl protons. For example in **5**, this consisted of one set of *ortho*-coupled aromatic protons (δ 6.80 and 7.06, each 1H, d, $J = 8.0$ Hz, H-4′ and H-5′, respectively) and two singlets (δ 6.76 and 6.94, each 1H, H-2 and H-5, respectively). Similar NMR spectral data were observed for **6**. Between the two possibilities for dimerization, C-4 to C-2′ or C-5 to C-2′, only the former was consistent with three-bond HMBC correlations observed in both **5** and **6** between H-7/C-5 and H-2/C-4. The very subtle differences between **5** and **6** could be attributed to the existence of stable atropisomers arising from hindered rotation at the biaryl bond due to the *ortho* substituents consisting of one hydroxyl and two methyl groups.

An additional set of closely related diastereomers, dicurcuphenols D (**7**) and E (**8**), co-eluted from C_{18} HPLC as an inseparable mixture. As compared with the downfield ^{1}H NMR spectra for **5** and **6** described above, the aryl resonances for **7** and **8** in Figure 2e were comprised of two sets of overlapping doublets. Furthermore, **7** and **8** were distinguished by the lack of singlet aromatic resonances characteristic of H-2 in **1** (Figure

1a). This unequivocally indicated the presence of a biaryl bond connectivity from C-2 to C-2′ in **7** and **8**. In analogy to the situation above, it was further concluded that each compound could exist as atropisomers, as there were now four *ortho* substituents present in the vicinity of the biaryl bond. Finally, the resonances for H-7and H-7′ (Figure 2e), as well as other upfield signals, provided insight as to the relative ratio of **7** to **8** in the mixture (~ 1:2.3, major isomer not defined here).

It was immediately evident that the final dimer isolated, dicurcuphenol ether F (**9**) was different than **4 – 8**. Dimer **9** exhibited five aromatic protons (Figure 2f), whereas the former five compounds all had four such protons. The aryl resonances in **9** consisted of two *ortho*-coupled protons, H-4 and H-5 (each d, J = 7.5 Hz) in addition to three singlet resonances. These data indicated the presence of tri- and tetra-substituted aryl rings connected in two possible ways: C-1 to C-4′, or C-1 to C-5′. The singlet at δ 6.32 (H-2) exhibited HMBC correlations to C-4, which with the above information, was key in defining the tri-substituted ring. Similarly, the tetra-substituted ring was delineated by the correlations between H-7′/C-5′, H-7′/C-1′, and H-15′/C-4′. The other two nearly overlapping singlets (δ ~6.67) were assigned by HMBC as H-2′ and H-5′. The three sets of data supporting the conclusion that **9** possessed the C-1 to C-4′ linkage were as follows. The similar shifts of **1** H-2 (δ 6.62) versus **9** H-2′ (δ 6.67) were consistent with an additional oxygen added to the *meta* and not *ortho* position in contrast to the large *ortho* effect differences in **1** H-5 (δ 7.05) versus **9** H-5′ (δ 6.67). Also, the nearly identical shifts of C-2′ (δ 118.0) and C-5′ (δ 118.8) meant that these carbons were *ortho* and *para* relative to both oxygen substituents. Finally, the three-bond HMBC correlations observed between H-5′/C-7′, H-15′/C-4′, and H-7′/C-1′ fixed H-5′ as being between C-6′ and C-4′.

Absolute Configuration Analysis and Laccase-Mediated Formation of Dicurcuphenols 4 – 9. With the planar structures of the dicurcuphenols established, the next challenge was to elucidate their absolute configurations. A key benchmark was the 7*S* absolute stereochemistry of (*S*)-(+)-curcuphenol (**1**), previously determined via total synthesis,[33,34,35] and the 7*R* stereoisomer, (*R*)-(-)-curcuphenol, also established by synthesis (Ono et al., 1995; Kimachi and Takemoto, 2001; Ono et al., 2001).[34,36,37] From

9

a biosynthetic perspective, it seemed reasonable to assume that **4 – 9** also possessed 7*S*, 7′*S* stereochemistry based on the co-occurrence of **1** with **4 – 9**.

As a logical extension of this observation, it can be hypothesized that the radical-mediated coupling of **1** would lead to the formation of dimers **4 – 9**. The steps in this process beginning with loss of H$^\bullet$ followed by reassembly of the various possible radical species are shown in Figure 4. Numerous organisms, particularly fungi, are known to possess phenol oxidase-type enzymes that are capable of catalyzing the polymerization of phenolic substrates under both natural and laboratory conditions.[38,39] The laccases, which are blue-copper oxidases, constitute one prominent class of phenol oxidases that have received widespread attention for their industrial applications.[40] Polyphenol oxidase (tyrosinase)[38] and horseradish peroxidase[41] represent other notable enzymes that carry out similar transformations.

Insert Figure 4

To test the above hypothesis, an experiment was undertaken with the goal of using **1** as a substrate for generating dimers. Accordingly, laccase, polyphenol oxidase, and horseradish peroxidase were surveyed in a set of preliminary experiments. The catalysis products were assessed by ESIMS analysis with success achieved in 13 out of 78 different experimental conditions employing laccase while the other enzymes proved ineffective. Summarized in Table 1 (and Table S1, Supplemental Data) are the conditions producing the desired [MH]$^+$ peak at *m/z* 435 ($C_{30}H_{43}O_2$). Not shown here are data demonstrating that similar results were obtained using a polyphenol oxidase-mimetic periodate oxidation system[42] and Fenton peroxidation.[43]

Scale-up biocatalysis accompanied by isolation of the target *m/z* 435 products afforded the series of compounds illustrated in Figure 4. All six dimers, **4 – 9**, were formed in varying relative amounts. Also tabulated are the relative percentages of these compounds isolated in this study from the sponge source. Each enzyme reaction product was identified by comparisons of their ^{1}H NMR and optical rotation data to that obtained for the sponge-derived compounds. We were amazed to note that: (i) all of the sponge-derived dicurcuphenols **4 – 9** were also produced by the laccase transformation of **1**, (ii)

no other dimers of **1** were detected, and (iii) the relative yield of the dimers obtained from laccase incubation were, with the exception of that for **4**, parallel to that from the sponge source (Figure 4). These data intimate that **4 – 9** may also be produced in the sponge by a radical-mediated coupling mechanism. Another important outcome of the results of Table 4 is the implications for bolstering the 7*S* stereochemical assignment proposed herein for the dicurcuphenols. The biocatalysis results clearly show that the 7*S* stereochemistry of **1** is maintained among dimeric products **4 – 9**.

Somewhat surprising is that despite numerous repeated re-isolations of compound **1** from sponges, it has not been previously reported to be accompanied by dimerized sesquiterpenes. Furthermore, a comprehensive study[5] on the microbial biotransformation products of curcuphenol and curcudiol resulted in the formation of a large number of functionalized analogs but no dimers were observed. Surprisingly, these experiments employed several fungi that are likely to be competent for the production of laccase or other phenol oxidases. By ESIMS, we detected dimers of **1** in the sponge crude extracts and also observed the long-term bench-top stability of compound **1** in a variety of solvents (MeOH, CH_2Cl_2, $CHCl_3$, and DMF) suggesting that **4 – 9** are not artifacts of our isolation procedures.

It is interesting to note that a similar oxidative coupling process has been proposed in the formation of the acylphenol dimers, giganteones A and B from the fruits of the Malaysian plant *Myristica gigantea* (Myristicaceae).[44] Further biosynthetic parallels can also be drawn to the formation of the biphenyl lichen metabolite, contortin, from *Psoroma contortum*[45] and cuparane-type sesquiterpene dimers, mastigophorenes, from the liverwort *Mastigophora diclados*.[46] The formation of complex polymeric tyrosine metabolites such as bastadins from *Ianthella* spp. sponges[47,48,49] and pulcherosine from sea urchin embryos[50] represent pertinent parallels to the metabolites observed in this study.

Up to this point, the absolute configuration of the biaryl axial chirality of atropisomers **5** and **6**, as well as **7** and **8,** still remained undefined. The former two compounds, and their acetyl and benzyl ester derivatives were oils that precluded X-ray analysis, while the latter two resisted all of our attempts at chromatographic separation. The chiroptical data we obtained on the purified isomers could not be further evaluated

because of a lack of appropriate reference compounds or applicable sets of empirical rules. Therefore, a sensitive and reference-independent spectroscopic technique was sought that could fulfill these required needs. Vibrational circular dichroism (VCD)[51] has developed in recent years as a powerful, but underutilized method and it seemed relevant to addressing the difficult assignment of the axial chirality for **5** and **6**. In fact, important proof-of-concept illustrations of the power of this technique to solve our problem reside in the absolute configuration determination by VCD of the cotton atropisomers (+)- and (-)-gossypol as *P* and *M*, respectively,[52] and in a VCD study of an unexpected atropisomerically stable 1,1-biphenyl.[53]

The superimposed IR and VCD spectra of atropisomers **5** and **6** shown in Figure 5 provides the key data to be applied in the stereochemical determination. As expected, the IR spectra for both atropisomers, are virtually identical except for the negligible contributions of minor impurities at ~1700 and 1025 cm^{-1}. In contrast, their VCD spectra contain important diagnostic bands between 1600 – 1425 cm^{-1}, which are of opposite inflection, arising from the axial chirality differences of this pair. Some of the remaining VCD bands are nearly superimposible due to the identical chiral alkyl side chains present in both compounds. Consistent with this trend are the appearance of the IR and VCD spectra for **1** shown in Figure 6. As expected, the IR spectra of **1**, **5**, and **6** are similar while the VCD spectra of **1** is rather featureless between 1600 – 1425 cm^{-1}. This latter point strengthens observation that this region contained peaks diagnostic of the *P/M* axial chirality. The region between 1400 – 1000 cm^{-1} includes features arising from both the *P/M* and 7*S* chiralities. The strong positive VCD intensity near 1300 cm^{-1} in **1**, **5**, and **6** is consistent with 7*S* chirality for this trio of compounds.

Insert Figures 5 and 6

The next step in completing the stereochemical analysis involved generating theoretical VCD spectra expected for the two configurational possibilities. However, the flexible nature of the biaryl alkyl side chains presented a complication because a large set of nearly isoenergetic solution phase conformations would need to be considered. As a simplification, the truncated atropisomer (*P*)-**10** (Figure 7) was selected for theoretical

analysis since it eliminates conformational flexibility, thus permitting the singular visualization of VCD effects arising from axial chirality. Calculations of VCD intensity at the DFT level were needed for the (*P*)-atropisomer only since the opposite (*M*)-**10** structure must exhibit a mirror image VCD spectrum of (*P*)-**10**.

Insert Figure 7

An additional step was needed in order to directly apply the calculated VCD spectra of model compound (*P*)-**10**, shown as the lower trace in Figure 8, to the stereochemical determination under consideration. Reanalysis of the VCD spectra for atropisomers **5** and **6** was carried out to isolate the spectral effects arising from axial chirality. This consisted of subtraction of the VCD spectrum of **6** from that of **5** and dividing by 2, and the resultant difference spectrum is shown in the upper trace of Figure 8. Focusing on the VCD spectral region between $1600 - 1400$ cm^{-1} in Figure 8, a comparison of the calculated spectrum for (*P*)-**10** to the difference spectrum (($VCD_5 - VCD_6$)/2 = $VCD_{difference}$) revealed striking similarities among their prominent features. The close correlation between these spectra is quite outstanding in view of the simplicity of the model system employed for this purpose. Therefore, it was unambiguously determined that **5** and **6** exhibit *P* and *M* axial chirality, respectively.

Insert Figure 8

Biological Activity and Modeling Studies of Curcuphenol Metabolites.
Studies on the cytotoxic effects of **1**, using our standard disk-diffusion assay,[28] revealed that it possessed potent, but non-specific activity against several murine and human cell lines including colon and breast. This was in accordance with previous bioactivity observations for analogs of **1**.[22] Compounds **2 – 9** were subsequently examined in this screen against the same cell lines, but were found to be completely inactive. In addition, all compounds were also examined in a bench-top brine shrimp assay[26] similar to that performed for **1**. Only **1** displayed potent activity, killing all brine shrimp within ~20

13

min ($LC_{50} = 0.63 \pm 0.04$ µg/mL), while **2 – 9** exhibited no lethality even after 24 h at 100 µg/mL.

Curcuphenol (**1**) was examined for its lipoxygenase inhibitory activity against both human 12-lipoxygenase (12-hLO) and 15-lipoxygenase (15-hLO). These enzymes represent important therapeutic targets for the development of novel pharmaceuticals for the treatment of cancer (12-hLO) and atherosclerosis (15-hLO).[54] Compound **1** exhibited potent, but non-selective inhibitory activity against both 12-hLO (IC_{50} 2.9 ± 0.4 µM) and 15-hLO (IC_{50} 1.6 ± 0.3 µM). All of the other six compounds isolated herein were tested against both lipoxygenases, but only dimer **4** tested positive in this assay as it possessed modest and equipotent activity against both 12-hLO (IC_{50} 11.6 ± 1.8 µM) and 15-hLO (IC_{50} 11.4 ± 2.5 µM). Not clear at this juncture are the structural features responsible for the inactivity of compounds **2**, **3**, and **5 – 9** as compared to **1** and **4**.

In further examining the lipoxygenase activity data and structures for **1** and **4**, we suspected that both functioned as redox type inhibitors. In our past experience, the structural signature for such activity was the presence of a phenolic head-group.[31] Using a fluorescence-based assay, it was determined that **4** did not reduce the active site ferric iron species while **1** exhibited a more modest reducing effect over a relatively extended timeframe. This suggested that **1** functioned through both competitive- and redox-based inhibition mechanisms while **4** was not redox active.

These concepts were further explored by means of molecular modeling analysis of the active site binding of **1** and **4**. A homology model of 15-hLO from rabbit 15-lipoxygenase (15-rLO) has recently been developed by which the docking behavior of inhibitors can be visualized.[55] This model system has been effectively employed for the in silico selection and experimental validation of potent (low mM) inhibitors of 15-hLO. Shown in Figure 9 are docking results for **1** calculated with GLIDE in the 15-hLO active site. As seen in the upper panel (Figure 9a), the hydroxyl moiety was predicted to adopt a preferred orientation >4.0 Å away from the active site iron atom and therefore would not be able to reduce the iron atom. In this model, hydrogen bonding was observed to occur between the OH group and active site residues Glu355 and Gln546. Since the active site iron can change the pKa of nearby ligands, deprotonated-**1** was also docked in the same manner-using GLIDE (Figure 9b). These conditions showed that the hydroxide

anion resided within 2.1 Å of the iron atom and should be capable of redox inactivation. These two supporting models help explain the 15-hLO inhibitory properties and weak redox activity observed for **1**. Further modeling studies (data not shown) performed with the weak, non-reductive inhibitor **4** suggested that this compound is too sterically restrained within the active site to function in a redox fashion.

Insert Figure 9

Summary. Bisabolene-type sesquiterpenes constitute a diverse assemblage of terrestrial- and marine-derived metabolites. These compounds have demonstrated promising biological effects in a variety of assay systems, but none appear to be under current consideration for preclinical development. In an effort to further probe the structural and biological relationships of these metabolites, ESIMS-guided isolation was used to obtain several new dimeric curcuphenol (**1**) derivatives that were examined for their cell cytotoxicity and lipoxygenase inhibitory activities. Dimerization of **1**, both in the sponge and through laccase biocatalysis, resulted in the general loss of activity across all assay systems examined in this study. Molecular modeling studies of **1** and **4** with 15-hLO provided intriguing evidence for the existence of multiple active site conformations of this compound resulting in a mixed inhibition profile.

The biogenic origin of dimers **4 – 9** is likely due to the oxidative coupling of **1** which can take place at more than one site. Atropisomeric dimers **5** and **6** provided an opportunity to explore the application of VCD spectroscopy in the absolute configuration determination of marine-derived metabolites. This study offered compelling evidence that VCD is a powerful technique that should find broad application in modern structure determination studies. We are currently engaged in a wider survey of bisabolene structural variants including higher molecular weight congeners. This should lead to further opportunities to discover novel structural themes and biological activities within this chemical family. The application of methodologies such as ESIMS in the structure discovery process will be crucial in making this assertion a reality.

EXPERIMENTAL SECTION

General Methods. All 1D- and 2D-NMR spectra were recorded in $CDCl_3$ (Cambridge Isotope Laboratories, Inc.) on Varian UNITY INOVA 500 instruments. Multiplicities of carbon resonances were confirmed by DEPT experiments. Low- and high-resolution ESIMS data were obtained on an Applied Biosystems Mariner Biospectrometry Workstation. Optical rotations were determined on a Jasco DIP 370 polarimeter using a 130 μL microcuvett. VCD measurements were performed using a *Chiralir* FT-VCD/IR spectrometer (BioTools, Inc., Wauconda, IL) with a liquid-nitrogen-cooled MCT-detector, which has been modified with two photoelastic modulators optimized at 1400 cm^{-1}.[56]

Chromatography materials and supplies were used as previously described.[31] Buffers and other chemicals for biocatalysis studies were obtained from Sigma-Aldrich and used without further purification. Laccase was a gift from L. T. Holst Jr. (Dexter Chemical L.L.C.) and used without further purification. Horseradish peroxidase and polyphenol oxidase were purchased from Research Organics and Worthington, respectively.

Animal Material. The sponge (UCSC collection number 00372) was collected by SCUBA from the region of New Britton, Papua New Guinea in 2000 and examined by R. M. N. Van Soest (Zoological Museum, University of Amsterdam, Amsterdam, The Netherlands) for taxonomic identification. The sponge (~2.3 kg wet weight) exhibited a massive, lobate morphology with a light pink to tan exterior and light yellow interior. The surface morphology of the organism was characterized as composed of convoluted grooves with a membraneous surface. The interior was fibrous featuring spicules in a chaotic composition. These features support that UCSC 00372 is a relatively rare specimen of *Didiscus aceratus* (Ridley and Dendy) (Halichondrida, Desmoxyidae)[27] (see Supplemental Data for underwater photo of the sponge). Immediately following collection, the sponge was soaked in EtOH-sea H_2O (1:1) for 24 hr after which the liquid was decanted and the sponge transported to UCSC. Upon arrival, the sponge was immediately immersed in MeOH and placed in cold storage at 4 °C until extracted. Voucher specimens have been retained at UCSC and the Amsterdam Zoological Museum (ZMAPOR 17712) for reference.

Extraction and Isolation. The sponge (UCSC 00372, 2.3 kg wet weight) was extracted with MeOH (1L, 3×) and MeOH-CH_2Cl_2 (1L, 3×). These extracts were combined yielding 29.5 g of brown oily residue. The total organic extract was dissolved in 800 mL MeOH-H_2O (9:1) and partitioned against hexane (800 mL, 3×). The aqueous MeOH extract was further diluted with H_2O (final 1:1, vol:vol) and partitioned against CH_2Cl_2 (800 mL, 3×). The CH_2Cl_2 extract (10.1 g) exhibited brine shrimp toxicity (100% lethality at 10 μg/mL) and as a result was chromatographed over silica gel (gradient 100% hexane to 100% acetone) providing fractions S1 (31 mg), S2 (7.83 g) S3 (1.22 g), S4 (370 mg), and S5 (331 mg). Brine shrimp toxic fraction S2 (100% lethality at 10 μg/mL) was purified by C_{18} LPLC (50 to 100% acetonitrile) yielding fractions B1 (1.73 g), B2 (5.02 g), B3 (105 mg), B4 (109 mg), and B5 (59 mg). All of the biological activity was associated with fraction B2 (100% lethality at 10 μg/mL) which was subsequently analyzed by MS and HPLC and found to contain a single major (~50% by mass) component that upon further HPLC purification (semiprep C_{18} HPLC, 80-100% acetonitrile) was identified as (*S*)-(+)-curcuphenol (**1**) ($[\alpha]^{25}_D$ = 30.7°, *c* 4.3, $CHCl_3$) by comparison to literature data.[6,7] Compound **1** was responsible for all of the observed brine shrimp toxicity (LC_{50} = 0.63 ± 0.04 μg/mL).

Based on a different bioassay lead for compound **1** (hLO inhibition, see Results and Discussion), all other fractions were examined by MS analysis to determine the presence of potential related chemical species for further biological evaluation. Fraction B1 exhibited an ion of *m/z* 253 [MH]$^+$ suggesting the presence of a dihydroxylated derivative. Further purification of B1 by C_{18} preparative HPLC (40-60% acetonitrile) and semipreparative HPLC (isocratic 30% acetonitrile) yielded a 40 mg 1:1 mixture of 10β-hydroxycurcudiol (**2**) and its C-10 epimer, 10α-hydroxycurcudiol (**3**).

Further evaluation of fraction B2 provided evidence for the presence of several putative dimeric derivatives (*m/z* 435 [MH]$^+$) that were targeted for purification. Accordingly, fraction B2 was subjected to C_{18} preparative HPLC affording fractions P1 (86mg), P2 (58 mg), P3 (2.89 g), P4 (18 mg), P5 (60 mg), P6 (31 mg), and P7 (18 mg). Fraction P3 was found comprised mainly of compound **1** (purity >95%). Fraction P5 was applied to a PTLC plate and developed with toluene-ethyl acetate (95:5). A band (27 mg) possessing a molecular weight of *m/z* 435 was further purified by C_{18} semipreparative

HPLC (isocratic 85% acetonitrile) yielding dicurcuphenol A (**4**). Similarly, fraction P6 was applied to PTLC (100% toluene) providing fractions T1 (17 mg) and T2 (15 mg) each possessing *m/z* 435. Both fractions T1 and T2 were purified by C_{18} semipreparative HPLC (isocratic 90% acetonitrile) affording 13 mg each of dicurcuphenols B (**5**) and C (**6**), respectively.

Fraction P8 was chromatographed by C_{18} semipreparative HPLC (isocratic 90% acetonitrile) yielding H1 (6 mg) and H2 (11 mg). Fraction H1 was further purified by C_{18} semipreparative HPLC (isocratic 90% acetonitrile) affording 5 mg of a 1:2.3 mixture of dicurcuphenols D (**7**) and E (**8**), respectively. Fraction H2 was also purified by C_{18} semipreparative HPLC (isocratic 90% acetonitrile) yielding 10 mg of dicurcuphenol ether F (**9**).

10α-Hydroxycurcudiol (3): clear oil; ^{1}H NMR (CDCl$_3$, 500 MHz) δ 7.04 (1H, d, *J* = 8.0 Hz, H-5), 6.73 (1H, d, *J* = 8.0 Hz, H-4), 6.67 (1H, s, H-2), 3.53 (1H, brd, *J* = 9.5 Hz, H-10), 3.23 (1H, sextet, *J* = 7.0 Hz, H-7), 3.26 (3H, s, H-15), 1.70, (2H, m, H-8 and/or H-9), 1.46 (1H, m, H-8 and/or H-9), 1.24 (1H, m, H-8 and/or H-9), 1.24 (3H, d, *J* = 6.5 Hz, H-14), 1.18 and 1.11 (each 3H, s, H-12 and H-13); ^{13}C NMR (CDCl$_3$, 125 MHz) δ 153.3 (C-1), 136.6 (C-3), 130.1 (C-6), 126.4 (C-5), 121.7 (C-4), 117.1 (C-2), 79.6 (C-10), 73.7 (C-11), 36.5 (C-8), 30.2 (C-7), 28.0 (C-9), 26.7 (C-12), 22.7 (C-13), 21.0 (C-14 and C-15); HRESIMS *m/z* 253.1800 [MH]$^+$ (calcd for $C_{15}H_{25}O_3$ 253.1804).

Dicurcuphenol A (4): clear oil; $[\alpha]^{25}_D$ = 61.5° (*c* 4.7, CHCl$_3$); ^{1}H NMR (CDCl$_3$, 500 MHz) δ 6.90 (1H, s, H-5), 6.87 (1H, s, H-5′), 6.68 and 6.67 (each 1H, s, H-2 and H-2′), 5.13 (2H, t, *J* = 7.0 Hz, H-10 and H-10′), 4.70 (2H, brs, OH), 3.03 (1H, sextet, *J* = 7.0 Hz, H-7), 3.00 (1H, sextet, *J* = 7.0 Hz, H-7′), 1.97 (6H, s, H-15 and H-15′), 1.94 (4H, m, H-9 and H-9′), 1.68 and 1.67 (each 3H, s, H-12 and H-12′), 1.67 (2H, m, H-8$_a$ and H-8$_a$′), 1.59 (2H, m, H-8$_b$ and H-8$_b$′), 1.56 and 1.51 (each 3H, s, H-13 and H-13′), 1.23 (6H, d, *J* = 7.0 Hz, H-14 and H-14′); ^{13}C NMR (CDCl$_3$, 125 MHz) δ 151.9 and 151.8 (C-1 and C-1′), 134.8 (C-4 and C-4′), 134.3 (C-3, C-3′), 132.1 and 132.0 (C-11 and C-11′), 130.1 (C-6′), 130.0 (C-6), 128.8 (C-5′), 128.5 (C-5), 124.7 (C-10 and C-10′), 116.6 (C-2 and C-2′),

37.4 and 37.3 (C-8 and C-8′), 31.8 (C-7′), 31.3 (C-7), 26.3 and 26.1 (C-9′, C-15, and C-15′), 25.8 (C-9, C-12, and C-12′), 21.4 (C-14′), 21.1 (C-14), 17.8 (C-13 and C-13′); HRESIMS m/z 435.3262 [MH]$^+$ (calcd for $C_{30}H_{43}O_2$ 435.3263).

Dicurcuphenol B (5): clear oil; $[\alpha]^{25}_D$ = 103.0° (c 1.0, CHCl$_3$); ^{1}H NMR (CDCl$_3$, 500 MHz) δ 7.06 (1H, d, J = 8.0 Hz, H-5′), 6.94 (1H, s, H-5), 6.80 (1H, d, J = 8.0 Hz, H-4′), 6.76 (1H, s, H-2), 5.15 (1H, t, J = 7.0 Hz, H-10′), 5.11 (1H, t, J = 7.0 Hz, H-10), 4.80 and 4.67 (each 1H, brs, OH), 3.09 (1H, sextet, J = 7.0 Hz, H-7′), 3.03 (1H, sextet, J = 7.0 Hz, H-7), 1.96 (3H, s, H-15′), 1.93 (3H, s, H-15), 1.93 (4H, m, H-9 and H-9′), 1.76 (2H, m, H-8$_a$ and H-8$_a$′), 1.67 (6H, s, H-12 and H-12′), 1.65-1.58 (2H, m, H-8$_b$ and H-8$_b$′), 1.56 and 1.52 (each 3H, s, H-13 and H-13′), 1.24 (3H, d, J = 7.0 Hz, H-14′), 1.22 (3H, d, J = 7.0 Hz, H-14′); ^{13}C NMR (CDCl$_3$, 125 MHz) δ 153.2 (C-1), 150.5 (C-1′), 136.5 (C-3), 134.6 (C-3′), 132.2 and 131.3 (C-11 and C-11′), 131.6 (C-6), 130.5 (C-6′), 129.5 (C-5), 127.1 (C-2′), 126.9 (C-4), 126.0 (C-5′), 125.0 (C-10′), 124.5 (C-10), 121.3 (C-4′), 117.7 (C-2), 37.2 (C-8), 36.9 (C-8′), 32.7 (C-7′), 31.3 (C-7), 26.5 (C-9′), 26.0 (C-9), 25.8 (C-12 and C-12′), 21.4 (C-14), 21.0 (C-14′), 19.9 (C-15′), 19.1 (C-15), 17.8 (C-13 and C-13′); HRESIMS m/z 435.3261 [MH]$^+$ (calcd for $C_{30}H_{43}O_2$ 435.3263).

Dicurcuphenol C (6): clear oil; $[\alpha]^{25}_D$ = 2.87° (c 1.6, CHCl$_3$); ^{1}H NMR (CDCl$_3$, 500 MHz) δ 7.08 (1H, d, J = 8.0 Hz, H-5′), 6.96 (1H, s, H-5), 6.82 (1H, d, J = 8.0 Hz, H-4′), 6.77 (1H, s, H-2), 5.13 and 5.12 (each 1H, t, J = 7.0 Hz, H-10 and H-10′), 4.85 and 4.65 (each 2H, brs, OH), 3.14 (1H, sextet, J = 7.0 Hz, H-7′), 3.00 (1H, sextet, J = 7.0 Hz, H-7), 1.96 (3H, s, H-15), 1.94 (4H, m, H-9 and H-9′), 1.93 (3H, s, H-15′), 1.68 and 1.66 (each 3H, s, H-12 and H-12′), 1.68 (2H, m, H-8$_a$ and H-8$_a$′), 1.56 (2H, m, H-8$_b$ and H-8$_b$′), 1.54 and 1.53 (each 3H, s, H-13 and H-13′), 1.26 (3H, d, J = 7.0, H-14′), 1.24 (3H, d, J = 7.0, H-14); ^{13}C NMR (CDCl$_3$, 125 MHz) δ 153.2 (C-1), 150.5 (C-1′), 136.6 (C-3), 134.6 (C-3′), 132.2 and 131.3 (C-11 and C-11′), 131.7 (C-6), 130.5 (C-6′), 129.6 (C-5), 126.9 (C-4 and C-2′), 125.7 (C-5′), 125.0 (C-10′), 124.5 (C-10), 121.4 (C-4′), 117.8 (C-2), 37.7 (C-8′), 37.3 (C-8), 31.9 (C-7′), 31.7 (C-7), 26.3 (C-9′), 26.2 (C-9), 25.8 (C-12

and C-12′), 21.1 (C-14), 21.0 (C-14′), 19.9 (C-15′), 19.0 (C-15), 17.8 and 17.7 (C-13 and C-13′); HRESIMS m/z 435.3262 [MH]$^+$ (calcd for $C_{30}H_{43}O_2$ 435.3263).

Mixture of Dicurcuphenols D and E (7 and 8): clear oil; $[\alpha]^{25}_D = -10.0°$ (c 0.3, CHCl$_3$); ^{1}H NMR (CDCl$_3$, 500 MHz) δ 7.16 (d, $J = 7.5$ Hz, H-5$_E$ and H-5$_E$′), 7.15 (d, $J = 7.5$ Hz, H-5$_D$ and H-5$_D$′), 6.89 (d, $J = 7.5$ Hz, H-4$_E$ and H-4$_E$′), 6.88 (d, $J = 7.5$ Hz, H-4$_D$, H-4$_D$′), 5.13 (m, H-10$_D$, H-10$_D$′, H-10$_E$ and H-10$_E$′), 4.75 and 4.74 (brs, OH), 3.13 (t, $J = 7.0$ Hz, H-7$_E$ and H-7$_E$′), 3.12 (t, J = 7.0 Hz, H-7$_D$ and H-7$_D$′), 1.954 (s, H-15$_D$ and H-15$_D$′), 1.946 (s, H-15$_E$ and H-15$_E$′), 2.02-1.98 (m, H-9$_D$, H-9$_D$′, H-9$_E$ and H-9$_E$′), 1.76-1.53 (m, H-8$_D$, H-8$_D$′, H-8$_E$ and H-8$_E$′), 1.67 (s, H-12$_D$, H-12$_D$′, H-12$_E$ and H-12$_E$′), 1.54 (s, H-13$_D$ and H-13$_D$′), 1.53 (s, H-13$_E$ and H-13$_E$′), 1.243 (d, $J = 6.5$ Hz, H-14$_E$ and H-14$_E$′), 1.240 (d, $J = 6.5$ Hz, H-14$_D$ and H-14$_D$′); ^{13}C NMR (CDCl$_3$, 125 MHz) δ 151.4 (C-1$_D$, C-1$_D$′, C-1$_E$, and C-1$_E$′), 135.7 (C-3$_D$, C-3$_D$′, C-3$_E$, and C-3$_E$′), 131.4 (C-6$_D$, C-6$_D$′, C-6$_E$, C-6$_E$′, C-11$_D$, C-11$_D$′, C-11$_E$, and C-11$_E$′), 127.8 (C-5$_D$ and C-5$_D$′), 127.6 (C-5$_E$ and C-5$_E$′), 124.8 (C-10$_D$, C-10$_D$′, C-10$_E$, and C-10$_E$′), 122.3 (C-4$_D$, C-4$_D$′, C-4$_E$, and C-4$_E$′), 119.6 (C-2$_D$, C-2$_D$′, C-2$_E$, and C-2$_E$′), 37.6 (C-8$_E$ and C-8$_E$′), 36.9 (C-8$_D$ and C-8$_D$′), 32.6 (C-7$_D$ and C-7$_D$′), 32.0 (C-7$_E$ and C-7$_E$′), 26.4 (C-9$_D$ and C-9$_D$′), 26.2 (C-9$_E$ and C-9$_E$′), 25.8 (C-12$_D$ and C-12$_D$′, C-12$_E$ and C-12$_E$′), 20.9 (C-14$_D$, C-14$_D$′, C-14$_E$, and C-14$_E$′), 19.4 (C-15$_D$, C-15$_D$′, C-15$_E$, and C-15$_E$′), 17.7 (C-13$_D$, C-13$_D$′, C-13$_E$, and C-13$_E$′); HRESIMS m/z 435.3260 [MH]$^+$ (calcd for $C_{30}H_{43}O_2$ 435.3263).

Dicurcuphenol Ether F (9): clear oil; $[\alpha]^{25}_D = 67.5°$ (c 0.7, CHCl$_3$); ^{1}H NMR (CDCl$_3$, 500 MHz) δ 7.13 (1H, d, $J = 7.5$ Hz, H-5), 6.79 (1H, d, $J = 7.5$ Hz, H-4), 6.673 and 6.666 (each 1H, s, H-2′ and H-5′), 6.32 (1H, s, H-2), 5.11 (2H, m, H-10 and H-10′), 4.55 (1H, brs, OH), 3.24 (1H, sextet, $J = 7.0$ Hz, H-7), 2.94 (1H, sextet, $J = 7.0$ Hz, H-7′), 2.19 (3H, s, H-15), 2.12 (3H, s, H-15′), 1.89 (4H, m, H-9 and H-9′), 1.74 (1H, m, H-8$_a$), 1.67 and 1.66 (each 3H, s, H-12 and H-12′), 1.59 (3H, m, H-8$_b$ and H-8′), 1.54 and 1.52 (each 3H, s, H-13 and H-13′), 1.25 (3H, d, $J = 7.0$ Hz, H-14), 1.17 (3H, d, $J = 7.0$ Hz, H-14′); ^{13}C NMR (CDCl$_3$, 125 MHz) δ 155.8 (C-1), 149.1 (C-1′), 148.2 (C-4′), 136.4 (C-3), 133.4

(C-6), 132.2 (C-6′), 131.8 and 131.3 (C-11 and C-11′), 128.3 (C-3′), 127.2 (C-5), 124.9 and 124.6 (C-10 and C-10′), 122.7 (C-4), 118.8 (C-5′), 118.0 (C-2′), 115.6 (C-2), 37.3 (C-8), 37.2 (C-8′), 32.0 (C-7), 31.7 (C-7′), 26.5 (C-9), 26.0 (C-9′), 25.8 (C-12 and C-12′), 21.4 (C-14), 21.2 (C-15 and C-14′), 17.8 (C-13 and C-13′), 16.0 (C-15′); HRESIMS m/z 435.3262 [MH]$^+$ (calcd for $C_{30}H_{43}O_2$ 435.3263).

Enzyme-Mediated Synthesis of Dicurcuphenols. Three enzymes, horseradish peroxidase, polyphenol oxidase, and laccase, were screened for their ability to catalyze the production of the dimeric dicurcuphenols from the monomeric **1**. Very little transformation to the desired dimeric species was observed among the horseradish peroxidase and polyphenol oxidase preparations. However, several laccase preparations (13 of 78 combinations of buffers, co-solvents, and mediators) were identified as capable of catalyzing this transformation (see Supplemental Data) and therefore this enzyme was selected for further scale-up studies.

Three, 1 L Erlenmeyer flasks were prepared each containing 150 mL of 100 mM citrate buffer (pH 5) and 50 mL of MeOH. The crude enzyme preparation (4 g) was gently stirred for 30 min in 50 mL of citrate buffer and allowed to settle for 2 min before use. The cloudy suspension was decanted to remove the insoluble solid residue and the supernatant divided equally among the three flasks. Compound **1** (1.5 g) was dissolved in 3 mL DMF and 500 mg of **1** distributed to each of the three flasks. The flasks were loosely capped with aluminum foil and placed on a rotary shaker at 150 rpm for 24 hr.

The flasks were removed and their contents pooled before extraction by partitioning with a mixture of ethyl acetate-*sec*-butanol (95:5) (200 mL, 3×). The organic layer was removed and dried over MgSO$_4$ yielding 1.6 g of crude extract. Analysis by ESIMS of this extract was performed giving evidence for the presence of dimers (m/z 435) of **1**. The extract was subjected to repeated C$_{18}$ HPLC and silica gel PTLC as outlined above yielding 608 mg of untransformed **1** and dicurcuphenols **4** (46 mg), **5** (22 mg), **6** (18 mg), 1:2.3 mixture of **7** and **8** (11 mg), and **9** (11 mg).

Periodate Oxidation of 1. A periodate oxidative catalytic resin was prepared as described[57] with minor modifications. Briefly, 2.5 g of Amberlite IRA-900 ion exchange resin was combined with 2 g NaIO$_4$ in 20 mL deionized H$_2$O and stirred overnight. The

liquid was decanted and an additional 2 g NaIO$_4$ in 20 mL deionized H$_2$O added. This was stirred for 6 h at room temperature. The resin was filtered and washed with H$_2$O, THF, and ethyl acetate before being dried in a desiccator. Dimerization of **1** was performed as described.[42,57,58]

Fenton Peroxidation of 1. Compound **1** was incubated with Fenton-type reagents as described.[43,59] Briefly, 5 mM of metal (Fe^{2+}, Cu^{2+}, and Mn^{2+}) salts were combined with 5 mM EDTA, 5 mg of **1**, and 1 mM H$_2$O$_2$ in a mixture of 0.1 M potassium phosphate buffer (pH 7.0) with acetonitrile (1:1, vol:vol). Reactions proceeded at 37 °C for 60 min at which time cold H$_2$O was added and the mixture extracted with diethyl ether.

Vibrational Circular Dichroism (VCD) Studies. Compounds **5** (0.23 M) and **6** (0.11 M) were dissolved in CDCl$_3$ and placed in CaF$_2$ cells (path length 98 μm) for analysis. Spectra were acquired over 10 h at a resolution of 4 cm^{-1}.

Calculations were performed on the model atropisomer (*P*)-**10** using Gaussian 03[60] at the DTF level (B3LYP functional and 6-31G(d) basis set). Vibrational frequencies were scaled by 0.97 and converted to Lorentzian bands with 6 cm^{-1} half-widths for comparison to experimental data. The truncated (*P*)-**10** lacking the alkyl tails was chosen for analysis due to its limited conformational flexibility and so as to eliminate the contribution of the C-7 chiral center, thereby providing a spectrum whose features were dependant solely on the C-2/C-4′ axial chirality. The scaled VCD spectra for **5** and **6** were subtracted from one another and the resultant difference spectrum aligned and visually compared with that generated for (*P*)-**10**.

Lipoxygenase Inhibition Assay. Human reticulocyte 15-lipoxygenase (15-hLO) and human platelet 12-lipoxygenase (12-hLO) were expressed and purified as previously described.[29,61] The IC$_{50}$ values for compounds **1** – **9** against these enzymes were determined as previously described with minor modifications.[29,62] Briefly, all inhibitors and enzyme substrates were dissolved in MeOH (1 mg/mL) and added to 2 mL buffer with 0.1% Triton-X under constant stirring. After a brief equilibration, 15-hLO (25 mM HEPES, pH 7.5) or 12-hLO (25 mM HEPES, pH 8) was added and the enzyme activity monitored based on the rate of diene product formation at 234 nm at room temperature.

Multiple data points inclusive of the 50% inhibitory concentration were acquired and the data fit to a simple saturation curve.

Redox Inhibition Studies. Characterization of a redox mode of inhibition of compounds against lipoxygenase was performed as previously described.[31] Briefly, the iron atom in the model lipoxygenase, soybean 15-lipoxygenase (15-sLO), was activated to the ferric species with 13-hydroperoxy-9(*Z*),11(*E*)-octadecadienoic acid (HPOD). The oxidation status of the 15-sLO was monitored by fluorescence (excitation: 280 nm; emission: 328 nm) while test compounds were added to the reaction cell containing 2 mL borate buffer (pH 9.2) at room temperature with constant stirring. A relative increase in the fluorescence signal intensity indicated a reduction of the 15-sLO active site iron.

Molecular Modeling Studies. The 15-hLO homology model was created using the Protein Local Optimization Program (PLOP, University of California, San Francisco) whereby conserved residues were aligned with the rabbit 15-lipoxygenase (15-rLO) template. Docking of **1** and deprotonated-**1** into the active site was performed using GLIDE. Active site Van der Waals forces were reduced and the ligand inserted. The protein was then relaxed about the ligand using PLOP. The resultant Ramachandran maps generated from the STRIDE database indicated all residues were within acceptable phi psi spaces. Compound **1** and its ion form were then redocked into the minimized protein active site and found to adopt chemically reasonable poses. Full details of these methods and creation of the 15-hLO homology model can be found in Chorny et al.[55]

Supplementary Data. Supplemental data associated with this article can be found, in the online version, at TO BE INSERTED.

References

[1] Fusetani, N.; Wolstenholme, H. J.; Shinoda, K; Asai, N.; Matsunaga, S.; Onuki, H.; Hirota, H. *Tetrahedron Lett.* **1992**, *33*, 6823.

[2] Butler, M. S.; Capon, R. J.; Nadeson, R.; Beveridge, A. A. *J. Nat. Prod.* **1991**, *54*, 619.

[3] Li, C.-J.; Schmitz, F. J.; Kelly, M. *J. Nat. Prod.* **1999**, *62*, 1330.

[4] Gulavita, N. K.; De Silva, E. D.; Hagadone, M. R.; Karuso, P.; Scheuer, P. J.; Van Duyne, G. D.; Clardy, J. *J. Org. Chem.* **1986**, *51*, 5136.

[5] El Sayed, K. A.; Yousaf, M.; Hamann, M. T.; Avery, M. A.; Kelly, M.; Wipf., P. *J. Nat. Prod.* **2002**, *65*, 1547.

[6] Wright, A. E.; Pomponi, S. A.; McConnell, O. J.; Kohmoto, S.; McCarthy, P. J. *J. Nat. Prod.* **1987**, *50*, 976.

[7] Fusetani, N.; Sugano, M.; Matsunaga, S.; Hashimoto, K. *Experientia* **1987**, *43*, 1234.

[8] Rodríguez, A. D.; Vera, B. *J. Org. Chem.* **2001**, *66*, 6364.

[9] Sullivan, B. W.; Faulkner, D. J.; Okamoto, K. T.; Chen, M. H. M.; Clardy, J. *J. Org. Chem.* **1986**, *51*, 5134.

[10] Harrison, B.; Crews, P. *J. Org. Chem.* **1997**, *62*, 2646.

[11] Peng, J.; Franzblau, S. G.; Zhang, F.; Hamann, M. T. *Tetrahedron Lett.* **2002**, *43*, 9699.

[12] Kitagawa, I.; Yoshioka, N.; Kamba, C.; Yoshikawa, M.; Hamamoto, Y. *Chem. Pharm. Bull.* **1987**, *35*, 928.

[13] Nakamura, H.; Kobayashi, J.; Ohizumi, Y.; Hirata, Y. *Tetrahedron Lett.* **1984**, *25*, 5401.

[14] Kassulke, K. E.; Potts, B. C. M.; Faulkner, D. J. *J. Org. Chem.* **1991**, *56*, 3747.

[15] D'Armas, H. T.; Mootoo, B. S.; Reynolds, W. F. *J. Nat. Prod.* **2000**, *63*, 1593.

[16] Freyer, A. J.; Patil, A. D.; Killmer, L.; Zuber, G.; Myers, C.; Johnson, R. K. *J. Nat. Prod.* **1997**, *60*, 309.

[17] Miller, S. L.; Tinto, W. F.; McLean, S.; Reynolds, W. F.; Yu, M. *J. Nat. Prod.* **1995**, *58*, 1116.

[18] McEnroe, F.; Fenical, W. *Tetrahedron* **1978**, *34*, 1661.

[19] Schmitz, F. J.; Michaud, D. P.; Hollenbeak, K. H. *J. Org. Chem.* **1980**, *45*, 1525.

[20] König, G. M.; Wright, A. D. *J. Nat. Prod.* **1997**, *60*, 967.

[21] Suzuki, T.; Kikuchi, H.; Kurosawa, E. *Chem. Lett.* **1980**, *10*, 1267.

[22] Valeriote, F.; Corbett, T.; LoRusso, P.; Moore, R. E.; Scheuer, P. J.; Patterson, G.; Paul, V.; Grindely, G.; Bonjouklian, R.; Pearce, H.; Stuffness, M. *Int. J. Pharmacog.* **1995**, *33 (Suppl.)*, 59.

[23] Nafie, L. A.; Freedman, T. B. In Circular Dichroism; Berova, N.; Nakanishi, K.; Woody, R. W., Eds.; Wiley-VCH: New York, 2000; 2nd Edition, pp 97-131.

[24] Berova, N.; Nakanishi, K.; Woody, R. W., Eds. Circular Dichroism, Wiley-VCH: New York, 2000; 2nd Edition.

[25] Berova, N.; Borhan, B.; Dong, J. G.; Guo, J.; Huang, X.; Karnaukhova, E.; Kawamura, A.; Lou, J.; Matile, S.; Nakanishi, K.; Rickman, B.; Su, J.; Tan, Q.; Zanze, I. *Pure Applied Chem.* **1998**, *70*, 377.

[26] Sam, T. W. In Bioactive Natural Products: Detection, Isolation, and Structure Elucidation; Colgate, S. M.; Molyneux, R. J., Eds.; CRC Press: Boca Raton, 1993, pp 441-456.

[27] Hooper, J. N. A. Systema Porifera: A Guide to the Classification of Sponges, Vol. 1; Hooper, J. N. A.; Van Soest, R. W. M., Eds.; Kluwer Academic: New York, 2002, pp 755-772.

[28] Valeriote, F.; Grieshaber, C. K.; Media, J.; Pietraszkewicz, H.; Hoffmann, J.; Pan, M.; McLaughlin, S. *J. Exp. Ther. Oncol.* **2002**, *2*, 228.

[29] Amagata, T.; Whitman, S.; Johnson, T. A.; Stessman, C. C.; Loo, C. P.; Lobkovsky, E.; Clardy, J.; Crews, P.; Holman, T. R. *J. Nat. Prod*. **2003**, *66*, 230.

[30] Carroll, J.; Jonsson, E. N.; Ebel, R.; Hartman, M. S.; Holman, T. R.; Crews, P. *J. Org. Chem*. **2001**, *66*, 6847.

[31] Cichewicz, R. H.; Kenyon, V. A.; Whitman, S.; Morales, N. M.; Arguello, J. F.; Holman, T. R.; Crews, P. *J. Am. Chem. Soc*. **2004**, *126*, 14910.

[32] Segraves, E. N.; Shah, R. R.; Segraves, N. L.; Johnson, T. A.; Whitman, S.; Sui, J. K.; Kenyon, V.; Cichewicz, R. H.; Crews, P.; Holman, T. R. *J. Med. Chem.* **2004**, *47*, 4060.

[33] Fuganti, C.; Serra, S. *J. Chem. Soc., Perkin Trans. 1* **2000**, 3758.

[34] Kimachi, T.; Takemoto, Y. *J. Org. Chem.* **2001**, *66*, 2700.

[35] Hagiwara, H.; Okabe, T.; Ono, H.; Kamat, V. P.; Hoshi, T.; Suzuki, T.; Ando, M. *J. Chem. Soc., Perkin Trans. 1* **2002**, 895.

[36] Ono, M.; Ogura, Y.; Hatogai, K.; Akita, H. *Tetrahedron: Asymmetry* **1995**, *6*, 1829.

[37] Ono, M.; Ogura, Y.; Hatogai, K.; Akita, H. *Chem. Pharm. Bull.* **2001**, *49*, 1581.

[38] Burton, S. G. *Curr. Org. Chem.* **2003**, *7*, 1317.

[39] Kobayashi, S.; Uyama, H.; Kimura, S. *Chem. Rev.* **2001**, *101*, 3793.

[40] Mayer, A. M.; Staples, R. C. *Phytochemistry* **2002**, *60*, 551.

[41] Veitch, N. C. *Phytochemistry* **2004**, *65*, 249.

[42] Antolovich, M.; Bedgood, D. R., Jr.; Bishop, A. G.; Jardine, D.; Prenzler, P. D.; Robards, K. *J. Agric. Food Chem.* **2004**, *52*, 962.

[43] Goldstein, S.; Meyerstein, D.; Czapski, G. *Free Rad. Biol. Med.* **1993**, *15*, 435.

[44] Pham, V. C.; Jossang, A.; Sévenet, T.; Bodo, B. *Tetrahedron* **2002**, *58*, 5709.

[45] Elix, J. A.; Jayanthi, V. K.; Jones, A. J.; Lennard, C. J. *Aust. J. Chem.* **1984**, *37*, 1531.

[46] Fukuyama, Y.; Asakawa, Y. *J. Chem. Soc., Perkin Trans. 1* **1991**, 2737.

[47] Jaspars, M.; Rali, T.; Laney, M.; Schatzman, R. C.; Diaz, M. C.; Schmitz, F.; Pordesimo, E. O.; Crews, P. *Tetrahedron* **1994**, *50*, 7367.

[48] Miao, S.; Andersen, R. J.; Allen, T. M. *J. Nat. Prod.* **1990**, *53*, 1441.

[49] Pordesimo, E. O.; Schmitz, F. J. *J. Org. Chem.* **1990**, *55*, 4704.

[50] Nomura, K.; Suzuki, N.; Matsumoto, S. *Biochemistry* **1990**, *29*, 4525.

[51] Freedman, T. B.; Cao, X.; Dukor, R. K.; Nafie, L. A. *Chirality* **2003**, *15*, 743.

[52] Freedman, T. B.; Cao, X.; Oliveira, R. V.; Cass, Q. B.; Nafie, L. A. *Chirality* **2003**, *15*, 196.

[53] Freedman, T. B.; Cao, X.; Nafie, L. A.; Kalbermatter, M.; Linden, A.; Rippert, A. J. *Helvetica Chim. Acta* **2003**, *86*, 3141.

[54] Dailey, L. A.; Imming, P. *Curr. Med. Chem.* **1999**, *6*, 389.

[55] Kenyon, V.; Chorny, I.; Holman, T.; Jacobson, M. *J. Med. Chem*., submitted.

[56] Nafie, L. A. *Appl. Spectrosc.* **2000**, *54*, 1634.

[57] Harrison, C. R.; Hodge, P. *J. Chem. Soc., Perkin Trans. 1* **1982**, 509.

[58] Fulcrand, H.; Cheminat, A.; Brouillard, R.; Cheynier, V. *Phytochemistry* **1994**, *35*, 499.

[59] Foppoli, C.; Coccia, R.; Blarzino, C.; Rosei, M. A. *Int. J. Biochem. Cell Biol.* **2000**, *32*, 657.

[60] Frisch, M. J.; Trucks, G. W.; Schlegel, H. B.; Scuseria, G. E.; Robb, M. A.; Cheeseman, J. R.; Montgomery, J. A, Jr.; Vreven, T.; Kudin, K. N.; Burant, J. C.; Millam, J. M.; Iyengar, S. S.; Tomasi, J.; Barone, V.; Mennucci, B.; Cossi, M.; Scalmani, G.; Rega, N.; Petersson, G. A.; Nakatsuji, H.; Hada, M.; Ehara, M.; Toyota, K.; Fukuda, R.; Hasegawa, J.; Ishida, M.; Nakajima, T.; Honda, Y.; Kitao, O.; Nakai, H.; Klene, M.; Li, X.; Knox, J. E.; Hratchian, H. P.; Cross, J. B.; Adamo, C.; Jaramillo, J.; Gomperts, R.; Stratmann, R. E.; Yazyev, O.; Austin, A. J.; Cammi, R.; Pomelli, C.; Ochterski, J. W.; Ayala, P. Y.; Morokuma, K.; Voth, G. A.; Salvador, P.; Dannenberg, J. J.; Zakrzewski, V. G.; Dapprich, S.; Daniels, A. D.; Strain, M. C.; Farkas, O.; Malick, D. K.; Rabuck, A. D.; Raghavachari, K.; Foresman, J. B.; Ortiz, J. V.; Cui, Q.; Baboul, A. G.; Clifford, S.; Cioslowski, J.; Stefanov, B. B.; Liu, G.; Liashenko, A.; Piskorz, P.; Komaromi, I.; Martin, R. L.; Fox, D. J.; Keith, T.; Al-Laham, M. A.; Peng, C. Y.; Nanayakkara, A.; Challacombe, M.; Gill, P. M. W.; Johnson, B.; Chen, W.; Wong, M. W.; Gonzalez, C.; Pople, J. A. Gaussian 03, Revision B.04, Gaussian, Inc., Pittsburgh PA, 2003.

[61] Holman, T. R.; Zhou, J.; Solomon, E. I. *J. Am. Chem. Soc.* **1998**, *120*, 12564.

[62] Finazzi-Agro, A.; Avigliano, L.; Veldink, G. A.; Vliegenthart, J. F. G.; Boldingh, J. *Biochim. Biophys. Acta* **1973**, *326*, 462.

Figure Legends

Figure 1. Structures of the bisabolene sesquiterpene (*S*)-(+)-curcuphenol (**1**) and derivatives (**2 – 9**) obtained from *Didicus aceratus* in this study.

Figure 2. Comparative partial ^{1}H NMR spectra of compounds **1** (panel 'a'), **4** (panel 'b'), **5** (panel 'c'), **6** (panel 'd'), **7** and **8** (panel 'e'), and **9** (panel 'f').

Figure 3. Significant HMBC correlations ($\rightarrow$) observed for dicurcuphenol A (**4**) and dicurcuphenol ether F (**9**).

Figure 4. Yields and proposed mechanism for the formation of dicurcuphenols A – F (**4-9**) from the sponge *Didicus aceratus* and laccase-mediated biocatalysis of (*S*)-(+)-curcuphenol (**1**).
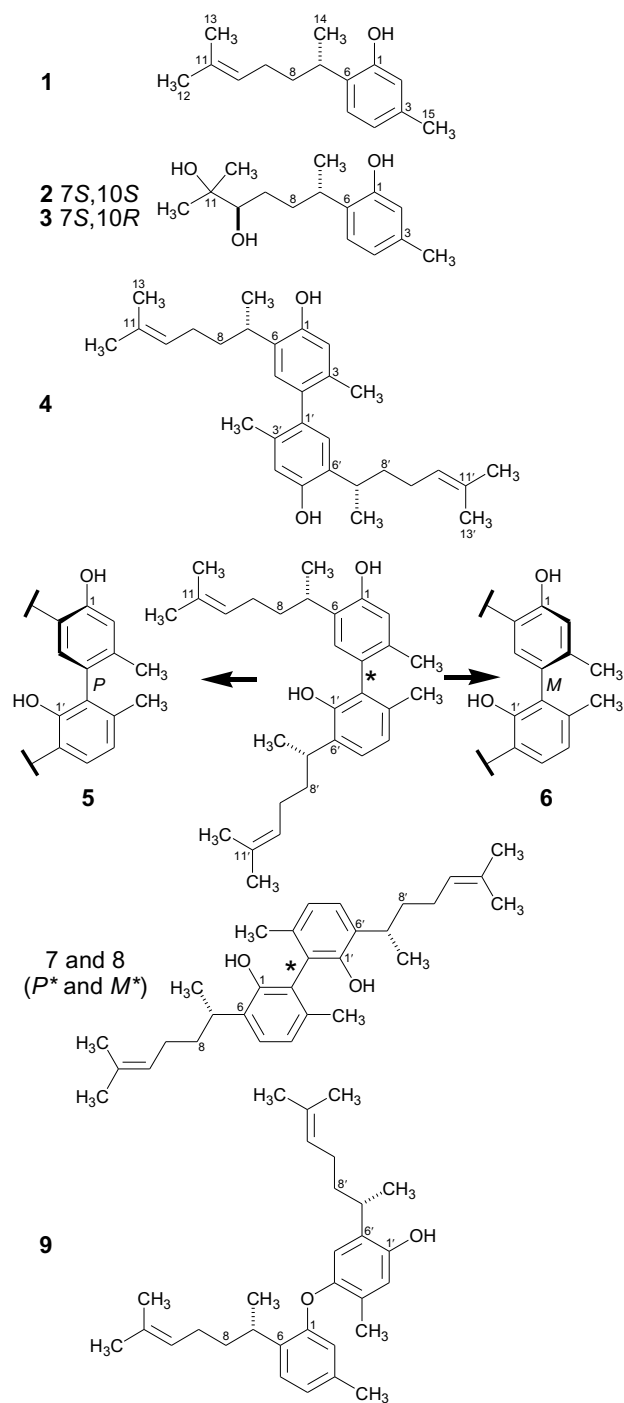
Figure 5. IR (lower traces) and VCD (upper traces, with VCD noise level shown above) spectra of **5** (red) and **6** (blue), in CDCl$_3$ solution. The IR spectra look quite similar with the exception of minor discrepancies around 1000 – 1050 cm^{-1} and 1700 cm^{-1} arising from impurities. Spectra are solvent subtracted.

Figure 6: IR (lower trace) and VCD (upper trace, with the VCD noise level shown above in red) spectra of monomer **1**, in CDCl$_3$ solution. Both spectra are solvent subtracted.

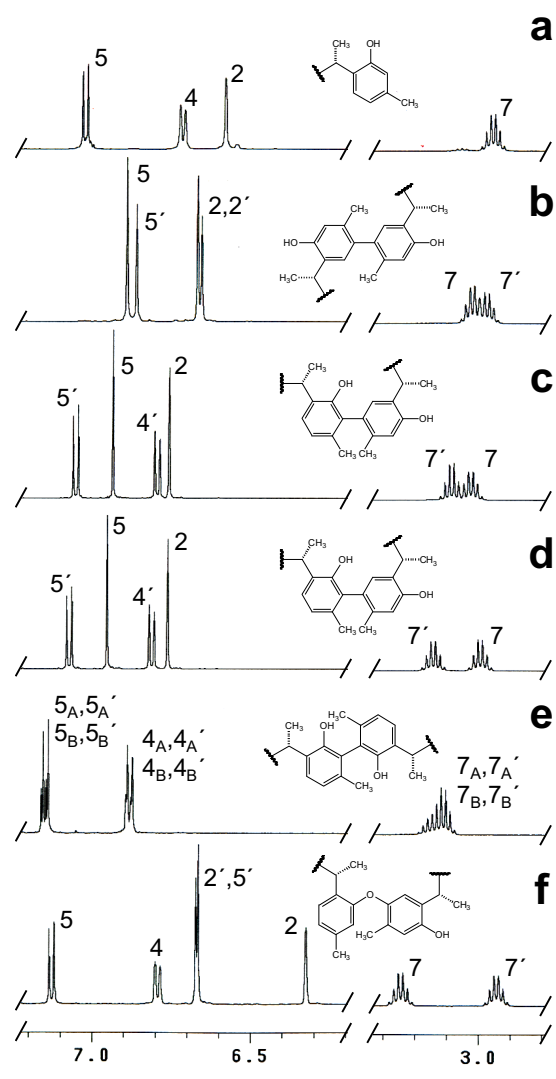**Figure 7.** Model phenol atropisomers (*P*)-**10** and (*M*)-**10** used for theoretical VCD calculations.

Figure 8. Observed (red, right axes) IR spectrum of **5** and difference VCD ((**5-6**)/**2**) vs. calculated (blue, left axes) spectra for the truncated model compound (*P*)-**10**. The observed spectra have been converted to molar absorptivities for direct comparison with the calculated spectrum.

Figure 9. Docking results for **1** (panel 'a') and deprotonated-**1** (panel 'b') in the active site of 15-hLO. Compound **1** is shown in blue with the active site iron identified as a yellow sphere.
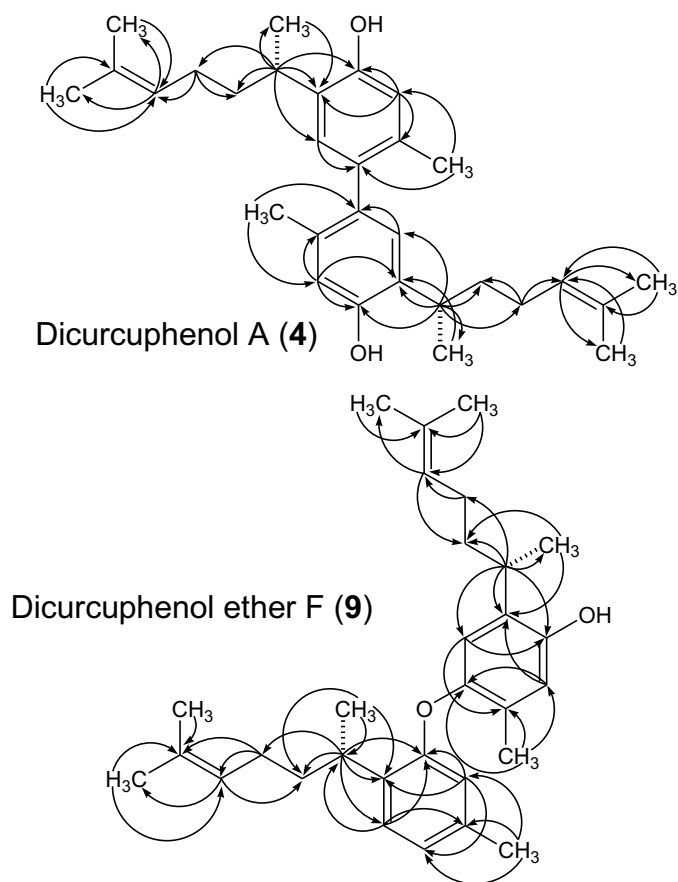
Figure 1. Structures of the bisabolene sesquiterpene (*S*)-(+)-curcuphenol (**1**) and derivatives (**2** − **9**) obtained from *Didicus aceratus* in this study.
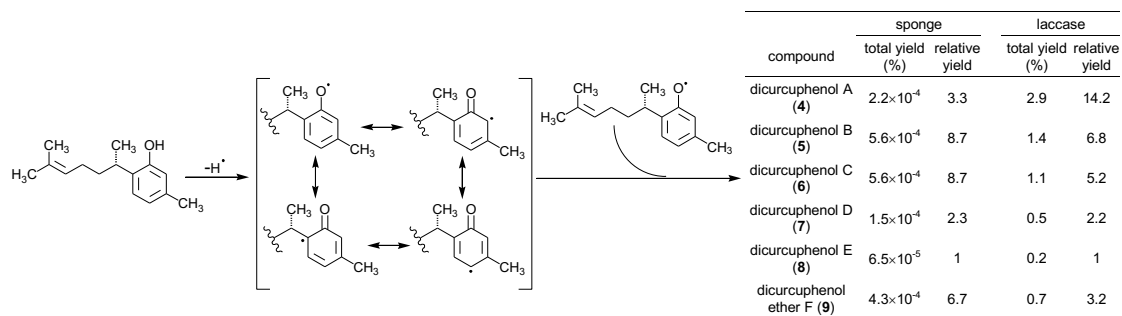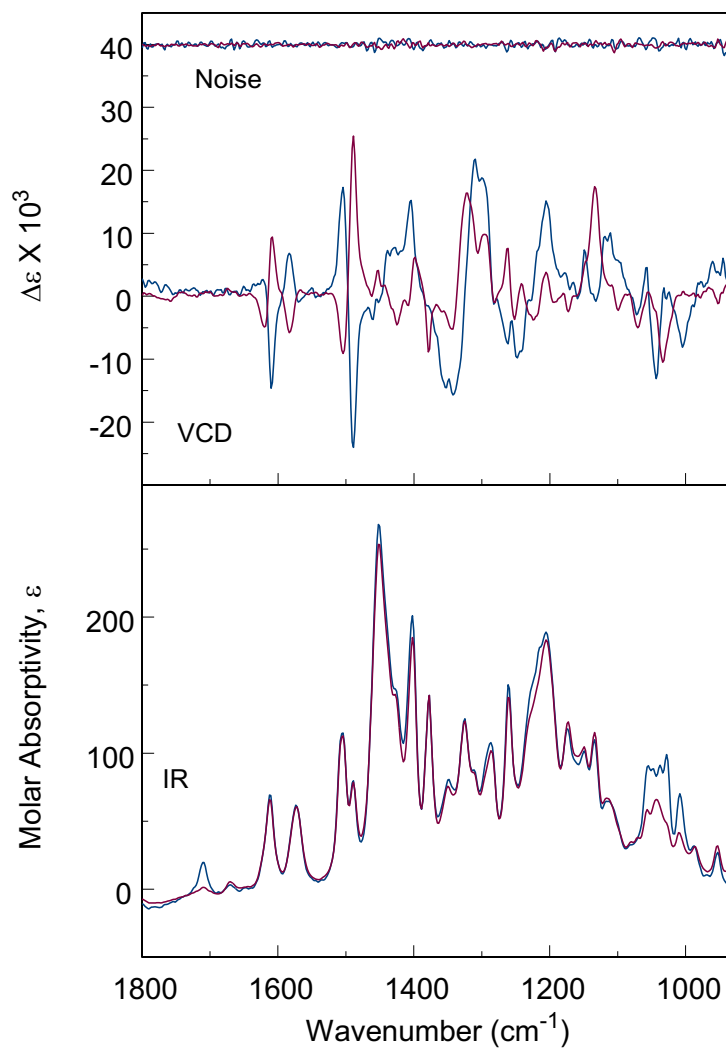
Figure 2. Comparative partial ^{1}H NMR spectra of compounds **1** (panel 'a'), **4** (panel 'b'), **5** (panel 'c'), **6** (panel 'd'), **7** and **8** (panel 'e'), and **9** (panel 'f').
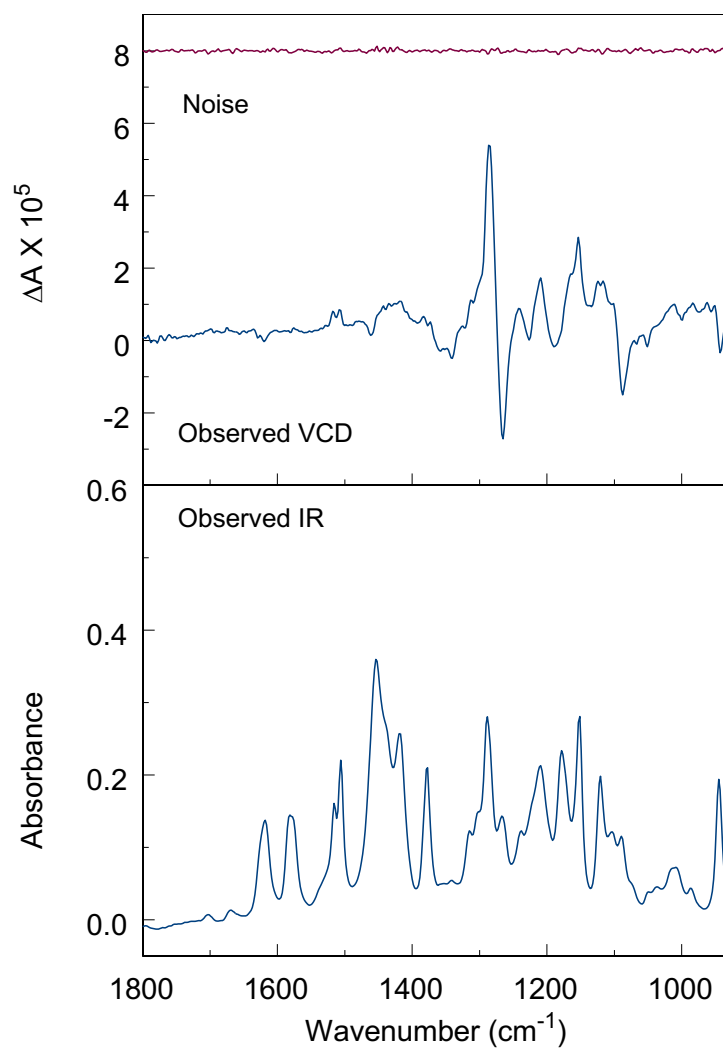
Figure 3. Significant HMBC correlations (→) observed for dicurcuphenol A (**4**) and dicurcuphenol ether F (**9**).

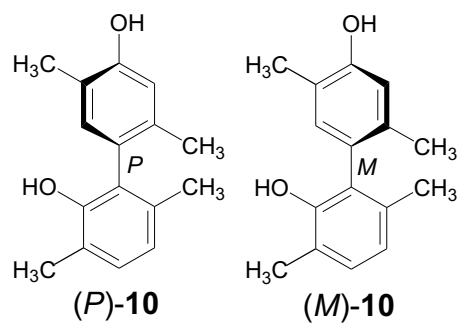| compound	sponge		laccase	
	total yield (%)	relative yield	total yield (%)	relative yield
dicurcuphenol A (4)	2.2×10^{-4}	3.3	2.9	14.2
dicurcuphenol B (5)	5.6×10^{-4}	8.7	1.4	6.8
dicurcuphenol C (6)	5.6×10^{-4}	8.7	1.1	5.2
dicurcuphenol D (7)	1.5×10^{-4}	2.3	0.5	2.2
dicurcuphenol E (8)	6.5×10^{-5}	1	0.2	1
dicurcuphenol ether F (9)	4.3×10^{-4}	6.7	0.7	3.2

Figure 4. Yields and proposed mechanism for the formation of dicurcuphenols A − F (**4** − **9**) from the sponge *Didicus aceratus* and laccase-mediated biocatalysis of (*S*)-(+)-curcuphenol (**1**).

Figure 5. IR (lower traces) and VCD (upper traces, with VCD noise level shown above) spectra of **5** (red) and **6** (blue), in CDCl₃ solution. The IR spectra look quite similar with the exception of minor discrepancies around 1000 – 1050 cm⁻¹ and 1700 cm⁻¹ arising from impurities. Spectra are solvent subtracted.

Figure 6: IR (lower trace) and VCD (upper trace, with the VCD noise level shown above in red) spectra of monomer **1**, in CDCl$_3$ solution. Both spectra are solvent subtracted.

Figure 7. Model phenol atropisomers (*P*)-**10** and (*S*)-**10** used for theoretical VCD calculations.
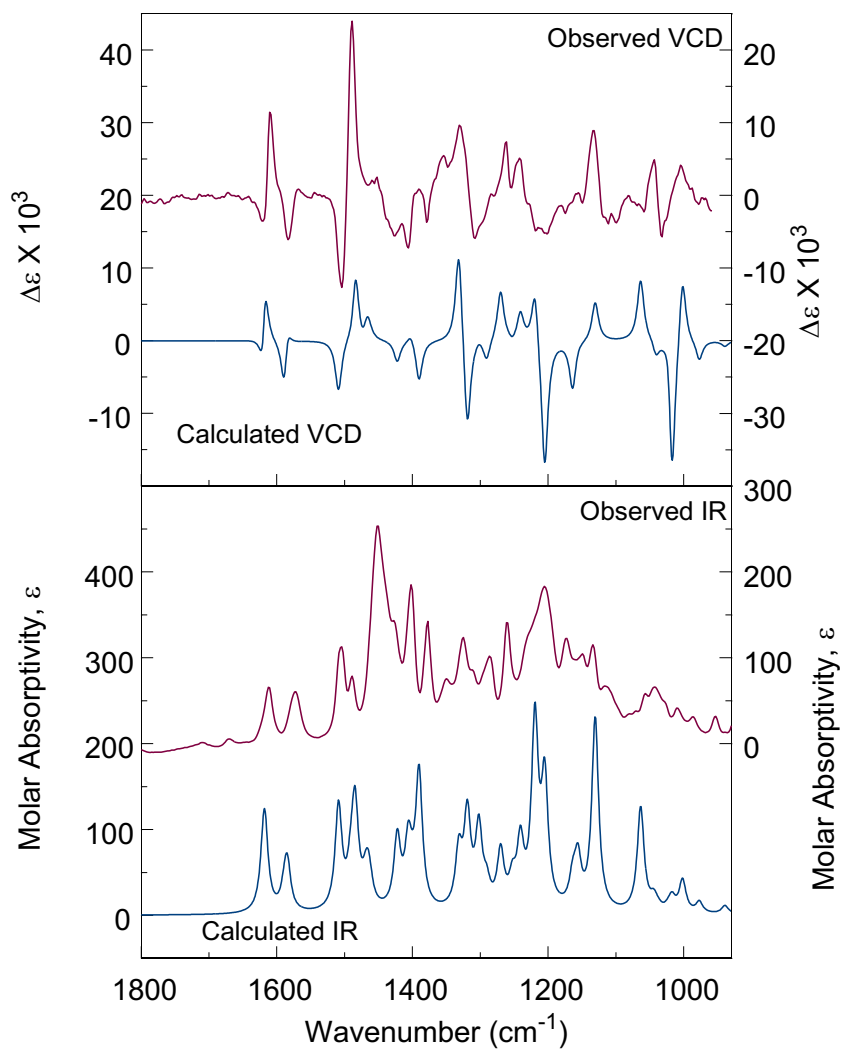
Figure 8. Observed (red, right axes) IR spectrum of **5** and difference VCD ((**5-6**)/**2**) vs. calculated (blue, left axes) spectra for the truncated model compound (*P*)-**10**. The observed spectra have been converted to molar absorptivities for direct comparison with the calculated spectrum.
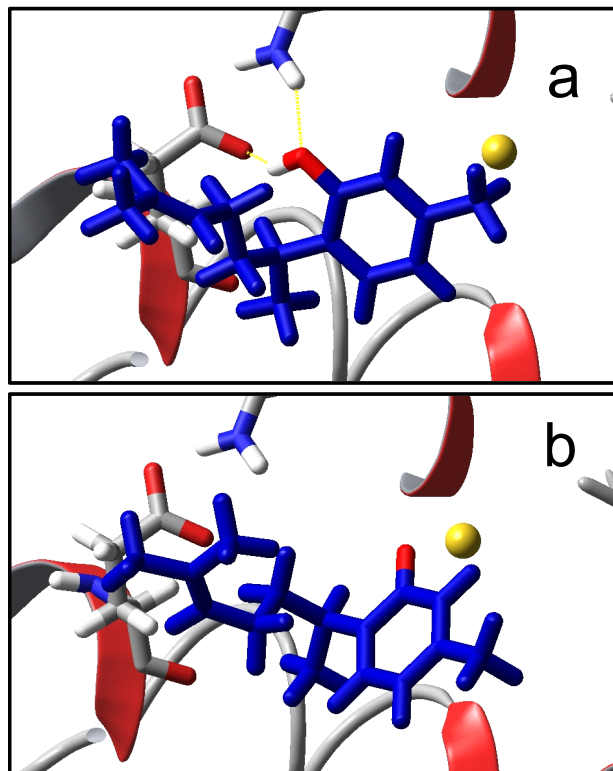
Figure 9. Docking results for **1** (panel 'a') and deprotonated-**1** (panel 'b') in the active site of 15-hLO. Compound **1** is shown in blue with the active site iron identified as a yellow sphere.

Table 1. Summary of mediators, buffers, and co-solvents tested in the laccase-mediated biocatalysis of curcuphenol (**1**) to dimers (ESIMS *m/z* 435). Items marked with an asterisk (*) were found to promote the transformation of compound **1**. See Table S1 in Supplemental Data for complete experimental details of 78 combinations tested.

Mediators	Buffers	Co-solvents
benzoic acid*	citrate (0.1 M, pH 5.0)*	acetone
catechol	potassium phosphate (0.1 M, pH 7.0)	acetonitrile*
hydroquinone*		butanol
4-methoxybenzoic acid*		benzene
4-methoxybenzoic acid polymer*		dimethylforamide*
phloroglucinol		dioxane*
tempo		ether
		ethanol*
		isopropanol*
		methanol*
		toluene
		triton X*